

Myelo-Enhancement by Astragalus Membranaceus in Male Albino Rats with Chemotherapy Myelo-Suppression. Histological and Immunohistochemical Study

Zeinab Mohamed Kamel Ismail, Noha Mohamed Afifi Amin,
Mira Farouk Youssef Yacoub, Amira Mohamed Osman Mohamed

Department of Histology, Faculty of Medicine, Cairo University, Cairo, Egypt

Background and Objectives: Myelo-suppression is the most common toxicity encountered in the oncology clinic today.

This study was planned to investigate the possible protective and therapeutic role of the traditional Chinese Medicinal Herb; Astragalus Membranaceus (AM), on chemotherapy-induced myelosuppression.

Methods and Results: This study was carried out on thirty six adult male albino rats. They were divided into: Group I Control Group (n=6) received a vehicle of phosphate buffered saline (PBS) solution. Group II (n=12) were injected I.P. with cyclophosphamide (CY) for 3 days (gIIa n =6) and continued for one more week to receive AM orally (gIIb n=6). Group III (n=6) received CY I.P. together with AM orally for 3 days. Group IV (n=12) received AM orally for one week (gIVa n=6) and continued for extra three days receiving CY I.P. with AM orally (gIVb n=6). Blood samples were analysed for Total Leucocytic Count and Lymphocytic Count. Counting of CD34 +ve cells in bone marrow was performed by flowcytometry. Bone marrow sections were subjected to H&E stain as well as immunohistochemical staining for anti- CD20 antibody. The mean area % of cellular bone marrow regions occupied by developing haemopoietic cells, mean area of fat cells and mean number of CD20 immunopositive B lymphocytes in the bone marrow were measured by histomorphometric studies and statistically compared. AM proved to have a myelo-protective and myelo-therapeutic capacity, evidenced at both laboratory and morphological levels.

Conclusions: The greatest myelo-potentiating effect of AM was achieved when supplied before and together with CY therapy.

Keywords: Myelo-suppression, Cyclophosphamide, CD34, CD20, Astragalus Membranaceus

Introduction

Myelo-suppression is the most common adverse effect

of cytotoxic chemotherapy, characterized by a decrease in blood cells production. Myelo-suppression remains the most common toxicity encountered in the oncology clinic today and this complication is likely to remain a serious problem indefinitely (1).

Cyclophosphamide (CY) is the most widely used alkylating agent in chemotherapy that acts by slowing or stopping cell growth (2).

There are no effective methods to treat myelo-suppression once it occurs. Blood transfusion can be effective in replenishing red blood cells and platelets but it doesn't improve white blood cell level (3).

An alternative to transfusion is haemopoietic growth

Accepted for publication March 20, 2014, Published online May 30, 2014

Correspondence to **Noha Mohamed Afifi Amin**

Department of Histology, Faculty of Medicine, Cairo University,
Cairo, 14 Akhaa buildings, Maadi, Cairo, Egypt

Tel: +201069626557

E-mail: noha_afifi@windowslive.com

© This is an open-access article distributed under the terms of the Creative Commons Attribution Non-Commercial License (<http://creativecommons.org/licenses/by-nc/3.0/>), which permits unrestricted non-commercial use, distribution, and reproduction in any medium, provided the original work is properly cited.

factors (HGFs) injection using colony stimulating factors (CSFs). These growth factors are natural chemicals that boost bone marrow performance and can accelerate haemopoietic recovery during cancer therapy. However, HGFs may not only stimulate the recovery of normal haemopoietic cells but also enhance the viability of tumor cells (4). Bone marrow transplant could be needed where the damaged bone marrow is beyond self-repair, but it is restricted by the few number of donors (5).

For these reasons, in the past several years, some experimental studies have been carried out in China, to evaluate the effects of Chinese herbal medicines (CHM) in preventing and treating chemotherapy-induced myelo-suppression (6).

Astragalus Membranaceus (AM) is one of the traditional Chinese medicines, approved by the State Food and Drug Administration of the People's Republic of China in 1999. AM acts by enhancing immune functions (7). It appears to exert its immunomodulatory actions via direct interaction with cellular membrane receptors. It has been reported that Astragalus root polysaccharide fractions could activate mouse B cells and stimulate macrophage production (8).

This study was planned to investigate the possible protective and therapeutic role of the traditional Chinese Medicinal Herb; Astragalus Membranaceus, on the bone marrow of chemotherapy-treated rats, monitored by laboratory, histological and immunohistochemical methods.

Materials and Methods

Material

Drugs:

- Cyclophosphamide (CY) (Trade name Endoxan), was purchased from Baxter Oncology GmbH, Halle, Germany, in the form of a vial 200 mg. The drug was dissolved in 10ml phosphate buffered saline (PBS) solution and was given by intraperitoneal (I.P.) injection, at a dose of 50 mg/kg/day (6).

- Astragalus Membranaceus (AM) Extract (Traditional Chinese Medicinal Herbs), manufactured by NOW FOODS 395 S. Glen Ellyn Rd., Bloomingdale, IL 60108. Made in U.S.A. It is supplied in a capsule form. Each capsule contains 500 mg of dried extract of AM (root). Each capsule was dissolved in 5 ml PBS vehicle and was supplied orally, at a dose of 2.5 g/kg body weight by the use of a special blunt tipped syringe (6).

Animals: The study was conducted at the Animal House of Kasr Al Ainy School of Medicine, according to the guidelines for the Care and Use of Laboratory Animals.

Thirty six adult male albino rats (12 weeks old) were used in this experiment, their weights ranged from 180~200 (185±1.25) gram. They were fed ad libitum and allowed free access to water.

They were divided into the following groups:

- Group I (GI) Control Group included 6 rats that received a vehicle of PBS solution, in the same pattern and route of administration (oral and/or I.P.) as the corresponding experimental groups and subgroups.

- Group II (GII) included 12 rats which were injected I.P. with CY 50 mg/kg/day (0.5 ml for each rat) for 3 days. It was subdivided into:

gIIa: 6 rats were sacrificed the following day after receiving the last dose of CY.

gIIb: 6 rats continued for one more week to receive 2.5 g/kg/day AM extract orally (5 ml/day).

- Group III (GIII) included 6 rats which received CY I.P. (50 mg/kg/day) together with 2.5 g/kg/day AM orally for 3 days.

- Group IV (GIV) included 12 rats which all received 2.5 g/kg/day AM orally for one week.

It was subdivided into:

gIVa: 6 rats were sacrificed the following day after receiving the last dose of AM orally for one week.

gIVb: 6 rats continued for extra three days receiving 50 mg/kg/day CY by I.P. injection together with 2.5 g/kg/day AM orally.

Methods

Induction of Myelo-Suppression: Cyclophosphamide was solubilized in PBS in Histology Department, Faculty of Medicine, Cairo University. The solution was prepared and injected I.P. within 15 minutes of its preparation, at a dose of 50 mg/kg/day (6).

Laboratory Investigations:

- Retro-orbital blood samples were collected by capillary tubes for analysis of Total Leucocytic Count (TLC) and Lymphocytic Count (LC). This was performed in the Clinical Pathology Department, Kasr Al-Ainy Medical Hospital.

- Detection and Counting of haemopoietic stem cells using flowcytometry with CD34 antibody (a commonly used marker for haemopoietic progenitor cells of all lineages) (9). CD34 was measured in the bone marrow samples by flowcytometry in Kasr Al Ainy Hospital, Flowcytometry Unit, Clinical Pathology Department.

Histological Study: The animals were sacrificed using chloroform inhalation. Right femur bones were subjected to calcium extraction using 10% Ethylene Diamine Tetraacetic Acid (EDTA) for 8 days. Bones were cut trans-

versely at the mid-shaft, then specimens were dehydrated in ascending grades of alcohol (70%, 95%, 100%), cleared in xylene then were embedded into paraffin wax (in Histology Department, Faculty of Medicine, Cairo University). Paraffin blocks were cut at 5~7 μm thickness, using Leica rotator microtome (Germany).

Sections were subjected to the following stains:

- Hematoxylin and Eosin stain (10).
- Immunohistochemical staining for anti-CD20 antibody using the avidin biotin peroxidase complex technique. Sections were counterstained with Meyer's hematoxylin (11). CD20 positive cells showed brown cytoplasmic deposits.

Anti-CD20 is a mouse monoclonal antibody (Lab Vision Corporation Laboratories, CA 94539, USA, catalogue number C 8080).

CD20 is a commonly used marker for the various stages of differentiation of normal B lymphocytes. It is expressed on the surface of all B-cells starting from the late pro-B-cell development stage and progressively increasing in concentration till maturity (12).

Positive tissue control: Human lymphoma biopsy with liver lymphoid aggregates showed +ve immunostaining for CD20 in the form of brown cytoplasmic deposits.

Negative control: Additional specimens of bone marrow were processed in the same sequence but the primary antibody was not added and instead, PBS was added in this step. Omission of the primary antibody gave no staining reaction.

Morphometric Study

Using a Leica Qwin 500 LTD image analysis computer system, (Cambridge, UK), the following parameters were measured in 10 non overlapping fields for each specimen:

- Mean area % of cellular bone marrow regions occupied by developing haemopoietic cells. The area percent represented the % of the cellular bone marrow regions occupied by developing haemopoietic cells, which were outlined

and masked by a binary color to the area of the standard measuring frame. It was measured using an objective lens $\times 10$ i.e. a total magnification $\times 100$.

- Mean area of fat cells in bone marrow sections. From the interactive measurement menu, "measure area" was selected. The cursor of the mouse was used to draw the outline of fat in each field and then the total area of fat for the field was calculated. It was measured at a magnification $\times 100$ in 10 serial fields in each section.

- Mean number of CD20 immunopositive B lymphocytes in the bone marrow. The cursor of the mouse was used to count the number of CD20 +ve cells and the mean value of number of cells for each slide was obtained. It was measured at a magnification $\times 400$, using the interactive measure menu.

Statistical Analysis

All measurements were subjected to statistical analysis using Student T test and ANOVA test using (SPSS) software version 9 Chicago USA (13).

Results

Results of Laboratory Investigations

Total Leucocytic Count (TLC) (Table 1 & Fig. 1A):

A significant reduction in TLC was recorded in gIIa as well as gIIb, as compared to the control value. Yet, the value for gIIb was significantly increased, as compared to gIIa. The highest mean value for TLC was recorded for gIVa, while the least value recorded was for gIIa, both values represented a statistically significant difference, as compared to all other groups and subgroups. Thus, there was significant increase in the mean values of TLC in GIII and gIVb, as compared to gIIb.

Lymphocytic Count (LC) (Table 2 & Fig. 1B): The value of LC showed significant decrease in gIIa and gIIb, as compared to GI. Yet, the value for gIIb was significantly

Table 1. The mean values (\pm SD) of TLC in the blood of control and experimental groups

| Group | Subgroup | Mean \pm SD |
|-------|----------|--|
| GI | | $4.8 \times 10^3 \pm 0.26$ |
| GII | gIIa | $0.6 \times 10^3 \pm 0.18^{*\lambda}$ |
| | gIIb | $3.4 \times 10^3 \pm 0.19^{*\lambda\alpha}$ |
| GIII | | $4.2 \times 10^3 \pm 0.23^{\lambda\alpha\Box}$ |
| GIV | gIVa | $6.7 \times 10^3 \pm 0.26^{*\alpha}$ |
| | gIVb | $4.5 \times 10^3 \pm 0.19^{\lambda\alpha\Box}$ |

*p<0.05 as compared to GI, λ p<0.05 as compared to gIVa, α p<0.05 as compared to gIIa, \Box p<0.05 as compared to gIIb.

Table 2. The mean values (\pm SD) of LC in the blood of control and experimental groups

| Group | Subgroup | Mean \pm SD |
|-------|----------|--|
| GI | | $3.3 \times 10^3 \pm 0.26$ |
| GII | gIIa | $0.4 \times 10^3 \pm 0.14^{*\lambda}$ |
| | gIIb | $1.9 \times 10^3 \pm 0.29^{*\lambda\alpha}$ |
| GIII | | $2.8 \times 10^3 \pm 0.24^{\lambda\alpha\Box}$ |
| GIV | gIVa | $5.4 \times 10^3 \pm 0.38^{*\alpha}$ |
| | gIVb | $2.9 \times 10^3 \pm 0.37^{\lambda\alpha\Box}$ |

*p<0.05 as compared to GI, λ p<0.05 as compared to gIVa, α p<0.05 as compared to gIIa, \Box p<0.05 as compared to gIIb.

increased, as compared to gIIa. The highest mean value for LC was recorded for gIVa, while the least value recorded was for gIIa, both values represented a statistically significant difference, as compared to all other groups and subgroups. Accordingly, there was significant increase in the mean value of LC in the blood in GIII and gIVb when compared to gIIb.

Flowcytometry of CD34 Cells in the Bone Marrow (Table 3 & Fig. 1C): The mean percentage of bone marrow CD34 immunopositive cells showed a significant decrease

in gIIa, as compared to GI. There was significant increase in gIIb, GIII, gIVa and gIVb, all these values were statistically significantly different from the control. The highest value of the percentage of bone marrow CD34 immunopositive cells was recorded in gIVa and the lowest value was detected in gIIa.

Histological Results

Hematoxylin and Eosin-Stained Bone Marrow Sections:

No histological variations were demonstrated on examina-

Table 3. The mean values (±SD) of LCin the blood of control and experimental groups

| Group | Subgroup | Mean ±SD |
|-------|----------|------------------------------|
| GI | | 0.29%±0.0029 |
| GII | gIIa | 0.06%±0.0023* ^λ |
| | gIIb | 0.44%±0.0026* ^{λ α} |
| GIII | | 0.48%±0.0018* ^{λ α} |
| GIV | gIVa | 0.59%±0.0024* ^α |
| | gIVb | 0.50%±0.0031* ^{λ α} |

*p<0.05 as compared to GI, ^λp<0.05 as compared to gIVa, ^αp<0.05 as compared to gIIa.

Table 4. The mean values (±SD) of LCin the blood of control and experimental groups

| Group | Subgroup | Mean ±SD |
|-------|----------|-----------------------------|
| GI | | 33.4%±2.5 |
| GII | gIIa | 6.5%±2.0* ^λ |
| | gIIb | 16.8%±3.2* ^{λ α □} |
| GIII | | 21.6%±1.4* ^{λ α □} |
| GIV | gIVa | 45.1%±3.2* ^α |
| | gIVb | 23.7%±1.6* ^{λ α □} |

*p<0.05 as compared to GI, ^λp<0.05 as compared to gIVa, ^αp<0.05 as compared to gIIa, [□]p<0.05 as compared to gIIb.

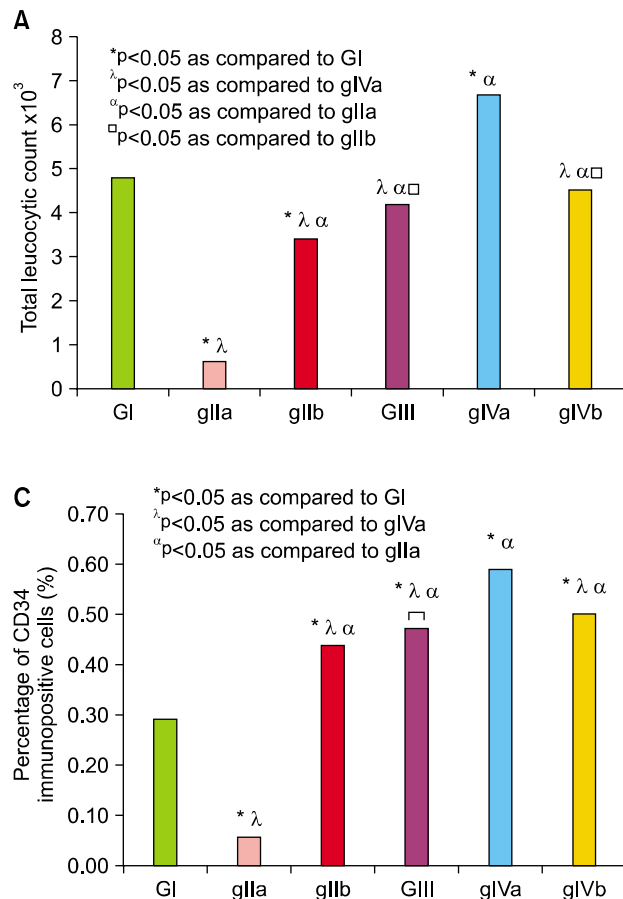


Fig. 1. (A) Comparing the mean values of TLC in the blood of control and experimental groups. (B) Comparing the mean values of lymphocytic count in the blood of control and experimental groups. (C) Comparing the mean values of the percentage of bone marrow CD34 immunopositive cells by flowcytometry. *p<0.05 as compared to GI, ^λp<0.05 as compared to gIVa, ^αp<0.05 as compared to gIIa, [□]p<0.05 as compared to gIIb.

tion of bone marrow sections of the different control groups. Histological examination of transverse sections (T.S) in the mid-shaft of femurs from the control group (GI) revealed normal bone marrow cellularity with heterogeneous populations of cells, at different stages of maturation. Developing haemopoietic stem cells; myeloid cells, erythroid cells, megakaryocytes as well as few macrophages could be demonstrated. Predominance of the developing myeloid series was observed. The developing cells

exhibited various outlines; some of which were spindle-shaped, while others appeared irregular in outline and showed mitotic figures. Blood sinusoids were lined by flat endothelial cells. Cells exhibiting pale nuclei belonging to the adventitial reticular cells were observed in the background of bone marrow sections (Fig. 2A).

Bone marrow sections of gIIa revealed very poor cellularity in relation to many wide marrow spaces. The minimal bone marrow cellularity included only few developing

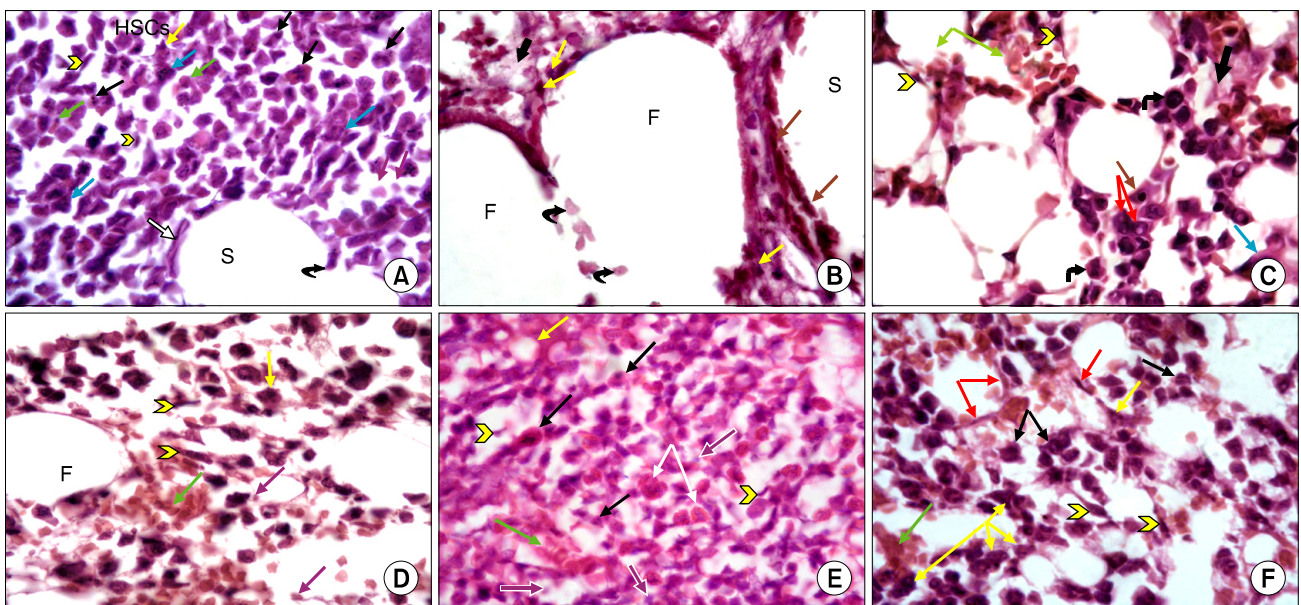


Fig. 2. (A) A photomicrograph of a transverse section (T.S) in the mid-shaft of femur from control group (GI) showing developing HSCs. Some cells are irregular in outline and show mitotic figures (black arrows), other cells are spindle-shaped (arrow heads). Different stages of myeloid cells are predominant, as well as erythroid cells (green arrows) in addition to megakaryocytes (blue arrows) and macrophages (yellow arrow). Pale nuclei in the background belong to adventitial reticular cells (purple arrows). A blood sinusoid (S) is demonstrated lined by endothelial cells (white arrow). Note interruption of the wall of the sinusoid by a cell passing through it (curved arrow) (H&E, $\times 1,000$). (B) A photomicrograph of a transverse section (T.S) in the mid-shaft of femur from gIIa showing BM cavities displaying large sized fat cells (F). A dilated blood sinusoid (S) is lined with hypertrophied endothelial cells (brown arrows). Several large branched cells containing engulfed black deposited material, probably macrophages, are seen (yellow arrows). Note the presence of acidophilic granular exudate material in the stromal background (thick arrow) and the presence of several damaged adventitial cells (curved arrows) (H&E, $\times 1,000$). (C) A photomicrograph of T.S in the midshaft of femur from gIIb showing improved bone marrow cellularity, with presence of more developing HSCs. Some of HSCs are spindle-shaped (arrow heads), others have irregular outline and exhibit large nuclei (curved arrows), while others exhibit pyknotic nuclei (brown arrow). Some cells show cytoplasmic vacuolations (red arrows). Note erythroid cells and RBCs (green arrows). Megakaryocyte (blue arrow) is the largest cell seen, characterized by having lobulated nucleus and abundant cytoplasm. Acidophilic exudate material is seen in the intercellular spaces (thick arrow) (H&E, $\times 1,000$). (D) A photomicrograph of T.S in the midshaft of a femur from gIII showing groups of developing HSCs; some of which are spindle shaped (arrow heads) and erythroid cells (green arrow), among oval shaped fat cells. Nuclei of the developing cells are large and darkly stained, while pale nuclei in the background belong to adventitial reticular cells (purple arrows). Note the presence of a multi-nucleated phagocytic cell (yellow arrow). A fat cell (F) is seen bounded by adventitial reticular and haemopoietic cells (H&E, $\times 1,000$). (E) A photomicrograph of T.S in the midshaft of femur from gIVa showing overcrowding of the bone marrow cavity with several developing HSCs exhibiting prominent nuclei. Many cells are spindle-shaped (arrow heads), others exhibit mitotic figures (black arrows). Numerous eosinophils are observed (white arrows). Spaces occupied by fat cells are small but clearly seen between HSCs (yellow arrow). Pale nuclei in the background belong to adventitial reticular cells (purple arrows). A longitudinal section in a small blood vessel is detected engorged with RBCs (green arrow) (H&E, $\times 1,000$). (F) A photomicrograph of T.S in the midshaft of femur from gIVb showing moderate population of bone marrow with developing HSCs, some of which are spindle-shaped (arrowheads), others show mitotic figures (black arrows). Blood sinusoids are seen lined by endothelial cells (red arrows), full with RBCs (green arrow) and WBCs, while macrophages (yellow arrows) are seen bordering blood sinusoids (H&E, $\times 1,000$).

HSCs, most of which exhibited pyknotic nuclei. The marrow spaces displayed expanded adipose tissue with large sized fat cells, as compared to the control group, as well as large sinusoidal spaces. The dilated sinusoids were lined with hypertrophied endothelial cells. In some fields, several large branched cells, "probably macrophages" were demonstrated, containing engulfed black deposited material. Several damaged adventitial cells as well as acidophilic exudate material were observed in the stromal background (Fig. 2B).

Bone marrow sections of gIIb showed signs of early recovery in the form of improved bone marrow cellularity with the presence of more developing HSCs of the myeloid, erythroid and megakaryocyte series and consequently, smaller fat cells, as compared to gIIa. The morphological appearance of the developing HSCs varied; some cells were spindle-shaped, others were irregular in outline and exhibited large nuclei, while the residual cells exhibited pyknotic nuclei. Moreover, cells with cytoplasmic vacuolations were displayed. Megakaryocytes were the largest cells observed in the marrow spaces, scattered be-

tween cellular components. Their lobulated nuclei and abundant cytoplasm were obvious (Fig. 2C).

Histological examination of T.S in the midshaft of femurs of GIII showed clumps of HSCs; myeloid as well as erythroid cells, deposited among the oval-shaped fat cells. Nuclei of the developing cells were large and darkly stained, while the pale nuclei observed in the background belonged to adventitial reticular cells. Multi-nucleated phagocytic cells were demonstrated in the stromal background. Fat cells were seen bounded by stromal, reticular and haemopoietic cells; myeloid & erythroid (Fig. 2D).

T.S. sections in the midshaft of femurs of gIVa showed high cellularity of the bone marrow. Islands of developing HSCs were seen over-crowded, filling the bone marrow cavities. Numerous eosinophils were observed in many fields. Spaces occupied by fat cells between HSCs were small, but yet clearly seen. Pale nuclei observed in the background belonged to adventitial reticular cells. Engorgement of small blood vessels with RBCs could also be demonstrated (Fig. 2E).

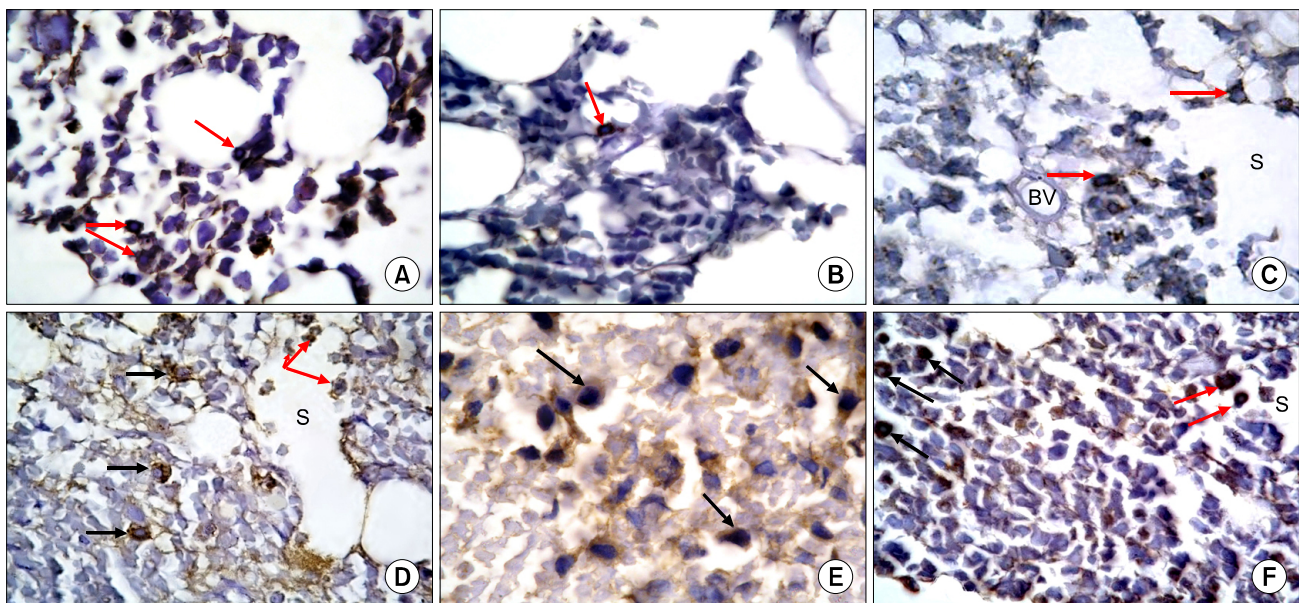


Fig. 3. (A) A photomicrograph of T.S in the midshaft of femur from the control group (GI) showing brown granular cytoplasmic immunoreactivity of some cells (arrows) (Anti-CD20 Immunostaining $\times 1,000$). (B) A photomicrograph of T.S in the midshaft of femur from gIIa showing a CD20 immunoreactive cell exhibiting brown cytoplasmic granules (arrow) (Anti-CD20 Immunostaining $\times 1,000$). (C) A photomicrograph of T.S in the midshaft of femur from gIIb showing CD20 immunoreactive cells exhibiting diffuse brown cytoplasmic granules (arrows). Note grouping of cells between a blood vessel (BV) and a blood sinusoid (S). (Anti-CD20 Immunostaining $\times 1,000$). (D) A photomicrograph of T.S in the midshaft of femur from GIII showing diffuse, brown granular cytoplasmic immunoreactivity in many cells (black arrows) closely related to blood sinusoid. Immunoreactive cells are also seen inside the lumen of a sinusoid (S), some are crossing the sinusoidal wall (red arrows) (Anti-CD20 Immunostaining $\times 1,000$). (E) A photomicrograph of T.S in the midshaft of femur from gIVa showing brown granular cytoplasmic immunoreactivity in many cells (arrows). Cells have rounded or oval nuclei (Anti-CD20 Immunostaining $\times 1,000$). (F) A photomicrograph of T.S in the midshaft of femur from gIVb showing diffuse brown granular cytoplasmic immunoreactivity of some cells (black arrows). Some of the cells (red arrows) are seen crossing the blood sinusoid (S) (Anti-CD20 Immunostaining $\times 1,000$).

Sections of gIVb showed moderate cellularity of the bone marrow. The bone marrow cavities contained developing HSCs, some of which exhibited pyknotic nuclei. Fat cells and acidophilic exudative material were demonstrated. Blood sinusoids were seen lined by flat endothelial cells and were engorged with many blood elements especially RBCs as well as WBCs, while macrophages were seen bordering blood sinusoids (Fig. 2F).

Immunohistochemical Results

Anti-CD 20 stained Bone Marrow Sections: Examination of anti-CD20 immunostained sections of the control group revealed some immunoreactive cells located inside the bone marrow cavities, closely related to the blood vessels as well as inside their lumina. Immunoreactivity was in the form of diffuse brown granular cytoplasmic reaction in some cells (Fig. 3A). Sections of gIIa showed very few CD20 +ve cells exhibiting brown granular cytoplasmic immunoreactivity (Fig. 3B), whereas sections of gIIb (Fig. 3C), GIII (Fig. 3D), gIVa (Fig. 3E) as well as gIVb (Fig. 3F) showed colonies of CD20 +ve cells exhibiting diffuse brown granular cytoplasmic immunoreactivity. Cells were closely related to blood vessels and blood sinusoids and some cells were seen crossing the walls of the blood sinusoids.

Quantitative Morphometric Results

Mean Area Percent of Cellular Bone Marrow Regions Occupied by Developing Haemopoietic Cells (\pm SD) in the studied groups: The value showed a significant decrease in gIIa, gIIb, GIII and gIVb. Yet, the value for gIIb was significantly increased, as compared to gIIa. On the other hand, a significant increase was detected in gIVa, as compared to GI. The highest mean area % of cellular bone marrow regions was recorded in gIVa and the lowest value was recorded in gIIa. Thus, there was significant increase in the mean area % of cellular bone marrow regions in

GIII and gIVb, as compared to gIIb (Table 4 & Fig. 4A).

Mean Area of Fat (\pm SD) in the studied groups: The value represented a significant increase in gIIa, as compared to GI. This value decreased significantly in gIIb, as compared to gIIa and decreased, but without significant difference, as compared to GI. The decrease in the mean area of fat represented a significant difference in GIII and gIVa, as compared to the control. The highest area of fat in bone marrow was recorded in gIIa and the lowest value was recorded in gIVa. Thus, there was significant decrease in the mean area of fat in bone marrow sections in GIII and gIVb when compared to gIIb (Table 5 & Fig. 4B).

Mean Number of CD20 Immunopositive Cells in Bone Marrow: The values recorded for all groups and subgroups represented a statistically significant difference, as compared to the control, with the exception of gIVb. Such difference was a significant decrease in gIIa, gIIb&GIII. On the other hand, it was a significant increase in gIVa, as compared to the control. The greatest number of CD20 immunopositive cells was recorded in gIVa and the least value was recorded in gIIa. Thus, there was significant increase in the mean number of CD20 immunopositive cells in GIII and gIVb when compared to gIIb (Table 6 & Fig. 4C).

Discussion

In the present work, the chosen chemotherapeutic agent for experimental induction of myelosuppression was CY, as several investigators reported the induction of bone marrow toxicity after the use of such drug. Experimental bone marrow suppression was induced by CY in normal adult Wistar rats (6). In human studies, hematologic profiles of CY-treated patients revealed anemia, leucopenia and/or thrombocytopenia (14).

Morphological signs of myelo-suppression could be clearly demonstrated on examination of bone marrow sec-

Table 5. The mean values (\pm SD) of area of fat cells in the control and experimental groups

| Group | Subgroup | Mean \pm SD |
|-------|----------|---|
| GI | | 2831.3 \pm 321 |
| GII | gIIa | 4428.0 \pm 699* ^{λ} |
| | gIIb | 3229.0 \pm 81 ^{λ} ^{α} |
| GIII | | 1977.6 \pm 233* ^{λ} ^{α} ^{\square} |
| GIV | gIVa | 571.6 \pm 138* ^{α} |
| | gIVb | 2364.3 \pm 367.7 ^{λ} ^{α} ^{\square} |

*p<0.05 as compared to GI, ^{λ} p<0.05 as compared to gIVa, ^{α} p<0.05 as compared to gIIa, ^{\square} p<0.05 as compared to gIIb.

Table 6. The mean number (\pm SD) of bone marrow CD20 immunopositive cells in the control and experimental groups

| Group | Subgroup | Mean \pm SD |
|-------|----------|--|
| GI | | 10.3 \pm 1.5 |
| GII | gIIa | 1.3 \pm 0.5* ^{λ} |
| | gIIb | 4.5 \pm 1.4* ^{λ} ^{α} |
| GIII | | 6.5 \pm 1.2* ^{λ} ^{α} |
| GIV | gIVa | 13.5 \pm 1.4* ^{α} |
| | gIVb | 9.5 \pm 1.0 ^{λ} ^{α} ^{\square} |

*p<0.05 as compared to GI, ^{λ} p<0.05 as compared to gIVa, ^{α} p<0.05 as compared to gIIa, ^{\square} p<0.05 as compared to gIIb.

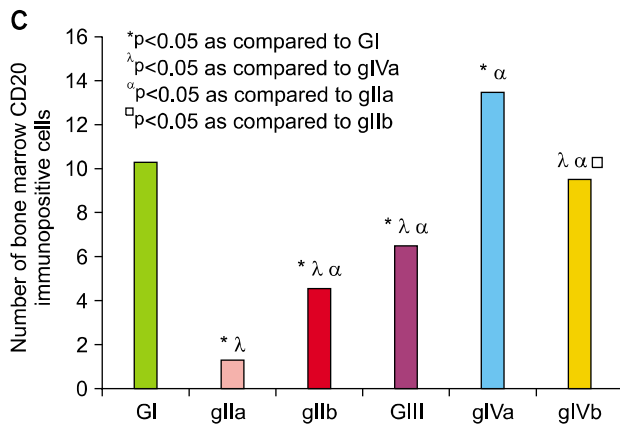
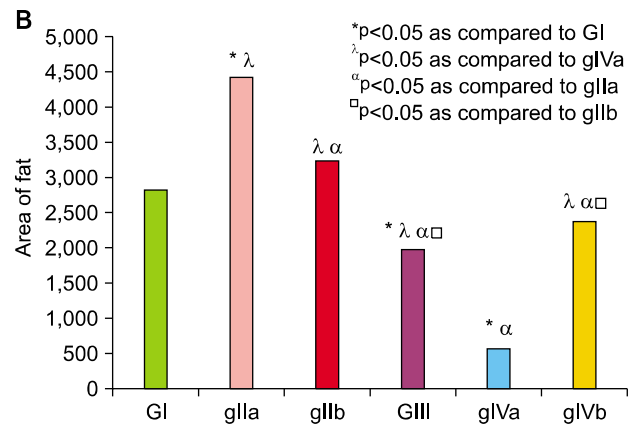
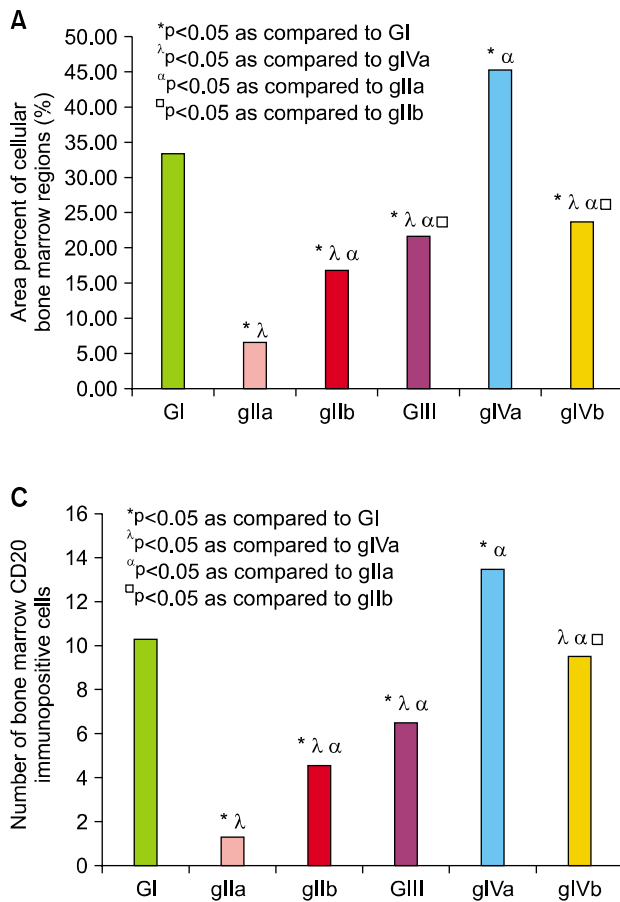


Fig. 4. (A) Comparing the mean values of mean area percent of cellular bone marrow regions. (B) Comparing the mean values of area of fat cells in the control and experimental groups. (C) Comparing the mean values of bone marrow CD20 immunopositive cells number in the control and experimental groups. *P < 0.05 as compared to GI, λ P < 0.05 as compared to gIVa, α P < 0.05 as compared to gIIa, □ P < 0.05 as compared to gIIb.

tions of CY-treated animals (gIIa). The occurrence of myelo-suppression was determined based on the detection of very poor marrow cellularity in relation to many wide marrow spaces. Few developing HSCs could be observed, most of which exhibited pyknotic nuclei. Similarly, other researchers reported that CY injection caused significant decrease in bone marrow cell counts (15).

The direct cytotoxic insult induced by the chemotherapeutic treatment might induce necrotic changes of the developing HSCs. The presence of necrotic tissue usually evokes an inflammatory response and eventually dead cells are phagocytosed by neutrophils and macrophages (16). Therefore, it was not surprising to detect the presence of large number of phagocytic cells, probably macrophages, containing engulfed deposited black material.

Several damaged adventitial cells were observed in the stromal background in sections of gIIa. Stromal cells of the bone marrow act as key regulators of haemopoiesis (17). Direct contact with some or all of these cells by HSCs may play a critical role in stem cell proliferation and differentiation. Studies by several laboratories suggest that several known growth-regulating factors and cytokines

may affect HSCs indirectly through effects on stromal cells (18). Thus, it seems reasonable that damage afflicted to the supporting stromal cells by the chemotherapeutic insult, would probably result in a microenvironment not suitable for supporting the developing HSCs and their subsequent necrosis.

In the present study, HSCs depletion observed in sections of gIIa went parallel with the biochemical parameters, by reporting a statistically significant reduction in TLC, as well as the LC in this group as compared to the control values, and recording the least value for these two parameters, as compared to all other groups and subgroups. HSCs depletion was further verified by morphometric measurements which revealed a significant decrease in the mean area % of cellular bone marrow regions occupied by developing haemopoietic cells in CY-treated group, compared to the control value, and recording the least value for this parameter, as compared to all other groups and subgroups.

Minimal bone marrow cellularity in sections of gIIa was associated with fat cell hypertrophy as well as sinusoidal dilatation. Stromal cells residing in the marrow spaces

give rise to cellular populations of the marrow micro-environment, such as osteoblasts and adipocytes. It is postulated that chemotherapy might induce a switch in the bone marrow stromal cells towards adipogenic differentiation at the expense of haemopoiesis (19). At the morphometric level, the highest area of fat in bone marrow sections was recorded in gIIa, representing a significant increase compared to all other groups and subgroups.

Sinusoidal dilatation observed in sections of gIIa might be caused by injury of endothelial lining due to chemotherapeutic regimen. This was verified by the presence of endothelial cells' hypertrophy. It has been proved previously that sinus endothelial cells are active in endocytosis and probably control passage of all materials into and out of the haemopoietic compartment (20). Based on our recorded results and the data from previous studies we can assume that the hypertrophy of sinusoidal endothelial cells might be due to enhanced endocytosis with disrupted exocytosis.

Bone marrow sections of rats which received CY followed by Astragalus (gIIb) showed signs of early recovery in the form of improved bone marrow cellularity with the presence of more developing HSCs of the erythroid, myeloid, and megakaryocyte series and consequently, smaller fat cells, as compared to gIIa. In addition, blood sinusoids were engorged with RBCs.

It has been previously reported that Astragalus could decrease apoptosis of bone marrow cells and could promote haemopoietic progenitor cells to differentiate along the erythroid and megakaryocyte line (21).

Moreover, the number of colony forming unit-megakaryocyte (CFU-Meg) was increased in anemic mice treated by Astragalus after chemotherapy, implying that this herb could accelerate the recovery of megakaryocyte haemopoiesis after bone marrow suppression (22).

Morphometric measurements revealed a significant increase in TLC & LC in gIIb, as compared to gIIa as well as the control group, with a corresponding significant increase in the mean area % of cellular bone marrow regions, and significant decrease in the mean area of fat as compared to CY treated sections.

When CY therapy was combined with Astragalus (GIII), groups of HSCs were seen gathered around blood sinusoids, among oval-shaped fat cells. Biochemical as well as morphometric analysis proved a significant increase of parameters in this "combined therapy" group, as compared to both gIIa and gIIb. It has been postulated that some physicians routinely provide chemotherapy patients with Astragalus; which seems to help the immune system differentiate between healthy cells and rogue cells, thereby

boosting the body's total cancer fighting system, thus improving the effectiveness of chemotherapy treatment. It also seems to stop the spread of malignant cancer cells to secondary healthy tissues (23).

Treatment with Astragalus alone (gIVa) achieved high bone marrow cellularity. Islands of developing HSCs were detected overcrowded filling the bone marrow cavities as well as engorgement of blood sinusoids with cellular elements. Numerous eosinophils were observed in many fields. Consequently, small sized fat cells were demonstrated. TLC & LC in gIVa achieved the highest value, as compared to all other groups and subgroups.

A significant increase of colony forming units of granulocytes, macrophages, erythroid cells, burst forming unit-erythroid cells, and megakaryocytes have been demonstrated following Astragalus therapy (24). Astragalus seems to have a dual effect; the "immune-modulating effect" directly increasing B lymphocytes, T lymphocytes, interleukin and antibody production, as well as the "adaptogenic effect" offering up viruses, bacteria and even cancer cells to be seen and recognized by the immune system (7).

Sections of gIVb which received Astragalus followed by chemotherapy combined with Astragalus, showed moderate cellularity of the bone marrow. It has been previously stated that Astragalus has been extensively used for clinical adjunctive therapy to ameliorate the side effects of antineoplastic drugs. Several clinical studies showed that the active constituents of Astragalus, including polysaccharides and flavonoids, could ameliorate the side effects of chemotherapeutic drugs (7). The presence of several macrophages in sections of gIVb indicates a stimulatory effect of Astragalus upon macrophages (25).

The ability of AM to stimulate bone marrow stem cells' proliferation was assessed in the present study by estimating the percent of bone marrow CD34+ve cells using flowcytometry. CD34+ve BM cells form a heterogeneous population of primitive stem cells and more mature progenitors committed to different lineages of differentiation (26). The highest value of the percentage of bone marrow CD34 immunopositive cells was recorded in gIVa (received Astragalus only). On the other hand, the lowest % of CD34 +ve cells was detected in gIIa (CY only). Previous investigations revealed that AM accelerated bone marrow haemopoietic stem progenitor cells in marrow-suppressed mice and enhanced cell proliferation by promoting cell cycles from G0/G1 phase to access into S, G2 phases (15).

The myelo-enhancing capabilities of Astragalus were valued, in the present work, not only at the level of pro-

moting bone marrow stem cells proliferation, but also at the level of encouraging their development into active immune cells. In that context, B lymphocytes were demonstrated by immunohistochemical staining using antibodies against CD20 antigen. On the other hand, very few CD20+ve cells could be demonstrated after treatment with CY alone (gIIa). The number of CD20+ve cells was markedly increased when Astragalus was given alone (gIVa), where colonies of CD20 +ve cells could be demonstrated. This was in accordance with morphometric analysis revealing the greatest number of CD20 immunopositive cells in gIVa (Astragalus only), whereas the least value was recorded in gIIa (CY only).

CD20 plays a role in human B cell proliferation and thus, CD20 expression was B cell restricted and was initiated during late pro-B cell development. The frequency and density of CD20 expression increased during B cell maturation in the bone marrow (27).

Conclusion

In this rat model of chemotherapy-induced myelosuppression, the Chinese Medicinal Herb "Astragalus Membranaceus" proved to have a myelo-protective and myelo-therapeutic capacity, which might be of considerable promise in the management of bone marrow toxicity.

Our findings provide experimental evidence ensuring the greatest effect of Astragalus medication, when supplied before and together with CY therapy. Meanwhile, it also proved its effectiveness in enhancing recovery of immunosuppression, if taken after CY therapy.

Myelo-enhancement potential of Astragalus in the current study was proved at both the *laboratory level* (evidenced by marked elevation of total leucocytic and lymphocytic counts and the number of CD34 +ve cells by flowcytometry), as well as the *morphological level* (evidenced by enhanced marrow cellularity).

Recommendations

In view of our findings on experimental rats, Astragalus is recommended as a promising agent for application in cancer immunotherapy, on condition that future human studies prove the same myelo-enhancing effects of Astragalus.

Further research studies are needed to estimate the immunomodulatory effect of the polysaccharides and other active ingredients of Astragalus on various immunodeficiency diseases. Further studies are also needed to examine the effect of Astragalus on other organs as spleen,

lymph node and thymus.

Potential conflict of interest

The authors have no conflicting financial interest.

References

1. Kuderer NM, Dale DC, Crawford J, Cosler LE, Lyman GH. Mortality, morbidity, and cost associated with febrile neutropenia in adult cancer patients. *Cancer* 2006;106:2258-2266
2. Pass GJ, Carrie D, Boylan M, Lorimore S, Wright E, Houston B, Henderson CJ, Wolf CR. Role of hepatic cytochrome p450s in the pharmacokinetics and toxicity of cyclophosphamide: studies with the hepatic cytochrome p450 reductase null mouse. *Cancer Res* 2005;65:4211-4217
3. Martín M, Lluch A, Seguí MA, Ruiz A, Ramos M, Adrover E, Rodríguez-Lescure A, Grosse R, Calvo L, Fernandez-Chacón C, Roset M, Antón A, Isla D, del Prado PM, Iglesias L, Zaluski J, Arcusa A, López-Vega JM, Muñoz M, Mel JR. Toxicity and health-related quality of life in breast cancer patients receiving adjuvant docetaxel, doxorubicin, cyclophosphamide (TAC) or 5-fluorouracil, doxorubicin and cyclophosphamide (FAC): impact of adding primary prophylactic granulocyte-colony stimulating factor to the TAC regimen. *Ann Oncol* 2006;17:1205-1212
4. Rades D, Fehlauer F, Bajrovic A, Mahlmann B, Richter E, Alberti W. Serious adverse effects of amifostine during radiotherapy in head and neck cancer patients. *Radiother Oncol* 2004;70:261-264
5. Lyman GH, Lyman CH, Agboola O. Risk models for predicting chemotherapy-induced neutropenia. *Oncologist* 2005;10:427-437.
6. Wang J, Tong X, Li P, Cao H, Su W. Immuno-enhancement effects of Shenqi Fuzheng Injection on cyclophosphamide-induced immunosuppression in Balb/c mice. *J Ethnopharmacol* 2012;139:788-795
7. Li J, Zhong Y, Li H, Zhang N, Ma W, Cheng G, Liu F, Liu F, Xu J. Enhancement of Astragalus polysaccharide on the immune responses in pigs inoculated with foot-and-mouth disease virus vaccine. *Int J Biol Macromol* 2011;49:362-368
8. Shao BM, Xu W, Dai H, Tu P, Li Z, Gao XM. A study on the immune receptors for polysaccharides from the roots of *Astragalus membranaceus*, a Chinese medicinal herb. *Biochem Biophys Res Commun* 2004;320:1103-1111
9. Macedo A, Orfão A, Vidriales MB, López-Berges MC, Valverde B, González M, Caballero MD, Ramos F, Martínez M, Fernández-Calvo J, et al. Characterization of aberrant phenotypes in acute myeloblastic leukemia. *Ann Hematol* 1995;70:189-194
10. Kiernan JA. *Histological and histochemical methods: theory and practice*. 3rd ed. London, New York & New Delhi: Arnold publisher; 2001. 111-162
11. Bancroft JD, Cook HC. *Immunocytochemistry*. In: *Manual of histological techniques and their diagnostic application*. 2nd ed. Edinburgh, New York: Churchill Livingstone; 1994.

- 263-325
12. Richard H. "Chapter 7: B Lymphocyte Development and Biology". In: Paul W, editor. *Fundamental Immunology*. 6th ed. Philadelphia, PA: Lippincott Williams & Wilkins; 2008. 237-269
 13. Armitage P, Berry G. In: Armitage, P, Berry G (Geoffrey), eds. *Statistical methods in medical reseach*. 3rd ed. London: Blackwell Scientific Publications; 1994. 12-48
 14. Haubitz M. Acute and Long-term Toxicity of Cyclophosphamide. *Transplantationsmedizin* 2007;19:26-31
 15. Zhao AB, Yu B, Wu XL, Cao KJ, Li EQ, Li QM, Chen XY. Protective effects on myelosuppression mice treated by three different classic Chinese medicine formulae. *Pharmacogn Mag* 2011;7:133-140
 16. Underwood JCE. Cellular injury in Part 1 of *General and Systemic pathology*, fourth edition, ElsevierInc, 2007. chapter 6: 105-107
 17. Ross M, Pawlina W. Bone marrow and formation of blood cells (haemopoiesis) In: *Histology: A Text and Atlas with Correlated Cell and Molecular Biology*. 6th ed. Baltimore, Philadelphia: Wolters Kluwer, Lippincott Williams & Wilkins; 2011. 289-300
 18. Liu S, Hu P, Hou Y, Li P, Li X, Tian Q. The additive effect of mesenchymal stem cells and bone morphogenetic protein 2 on γ -irradiated bone marrow in mice. *Cell Biochem Biophys* 2011;61:539-550
 19. McGuire TR, Brusnahan SK, Bilek LD, Jackson JD, Kessinger MA, Berger AM, Garvin KL, O'Kane BJ, Tuljapurkar SR, Sharp JG. Inflammation associated with obesity: relationship with blood and bone marrow endothelial cells. *Obesity (Silver Spring)* 2011;19:2130-2136
 20. Young B, Lowe J, Stevens A, Heath J. *Blood In: Wheater's Functional Histology. A Text and Colour Atlas*. 5th ed. Philadelphia, USA: Churchill Livingstone Elsevier; 2007. 42-61
 21. Lv Y, Feng X, Zhu B. Study on effect of Astragalus membranaceus injection on hematopoiesis in anemic mice with myelosuppression. *Zhong Yao Cai* 2005;28:791-793
 22. Zhu X, Zhu B. Effect of Astragalus membranaceus injection on megakaryocyte hematopoiesis in anemic mice. *Hua Xi Yi Ke Da Xue Xue Bao* 2001;32:590-592
 23. Wei H, Sun R, Xiao W, Feng J, Zhen C, Xu X, Tian Z. Traditional Chinese medicine Astragalus reverses predominance of Th2 cytokines and their up-stream transcript factors in lung cancer patients. *Oncol Rep* 2003;10:1507-1512
 24. Chen Y, Zhu B, Zhang L, Yan S, Li J. Experimental study of the bone marrow protective effect of a traditional Chinese compound preparation. *Phytother Res* 2009;23:823-826
 25. Cho WC, Leung KN. In vitro and in vivo immunomodulating and immunorestorative effects of Astragalus membranaceus. *J Ethnopharmacol* 2007;113:132-141
 26. Syrjälä M1 Ruutu T, Jansson SE. A flow cytometric assay of CD34-positive cell populations in the bone marrow. *Br J Haematol* 1994;88:679-684
 27. Uchida J, Lee Y, Hasegawa M, Liang Y, Bradney A, Oliver JA, Bowen K, Steeber DA, Haas KM, Poe JC, Tedder TF. Mouse CD20 expression and function. *Int Immunol* 2004;16:119-129